Journal of Theoretical Biology 268 (2011) 1–13

Contents lists available at ScienceDirect

Journal of Theoretical Biology

journal homepage: www.elsevier.com/locate/yjtbi

Modelling the effects of adherence to the HIV fusion inhibitor enfuvirtide

Jie Lou [a], Robert J. Smith? [b,*]

[a] Department of Mathematics, Shanghai University, 99 Shangda Road, Shanghai 200444, PR China
[b] Department of Mathematics and Faculty of Medicine, The University of Ottawa, 585 King Edward Avenue, Ottawa, Canada ON K1N 6N5

ARTICLE INFO

Article history:
Received 16 February 2010
Received in revised form
24 September 2010
Accepted 27 September 2010
Available online 1 October 2010

Keywords:
Enfuvirtide
Fusion inhibitors
Antiretroviral therapy
Mathematical model
Adherence

ABSTRACT

Recently, the first drug in a new class of antiretroviral HIV drugs was approved, the fusion inhibitor enfuvirtide. We develop a mathematical model that describes the binding of the virus to T cells. We model the effect of enfuvirtide upon this process using impulsive differential equations. We find equilibria and determine stability in the case of no therapy and then when therapy is taken with perfect adherence. We determine analytical thresholds for the dosage and dosing intervals to ensure the disease-free equilibrium remains stable. We also explore the effects of partial adherence. Our theoretical results suggest that partial adherence may, at times, be worse than no therapy at all, but at other times may in fact as good as perfect adherence. It follows that patients should be counselled on the importance of adherence to this new antiretroviral drug.

1. Introduction

Enfuvirtide (formerly T-20) is the first fusion inhibitor to be approved by the US Food and Drug Administration for the treatment of chronic human immunodeficiency virus (HIV) infection in adults and children 6 years and older (Hardy and Skolnik, 2004). Enfuvirtide is an injectable fusion inhibitor, and has demonstrated potent antiretroviral activity and excellent tolerability in extensively pre-treated patients (Liu et al., 2005; Moyle, 2003). The metabolism of enfuvirtide is not likely to be affected by coadministered medications, including ritonavir or a saquinavir–ritonavir combination, and is not itself expected to affect the metabolism of other coadministered drugs, suggesting a low potential for metabolic drug–drug interactions involving enfuvirtide (Castagna et al., 2005; Clotet et al., 2004).

HIV fusion with $CD4^+$ T cells is a complex process involving three stages (Liu et al., 2005; Levy, 2007). (1) The gp120 molecule of HIV first interacts with the CD4 receptor of the target cell. Heparan sulfate proteoglycan stabilises the interaction of the gp120 with CD4 receptor. (2) This interaction induces a conformational change in the gp120-exposing sites that interact with the chemokine receptor (CCR5 or CXCR4) on the surface of the T cell. This further stabilises the interaction, and the virus fusion protein (gp41) is uncovered and also undergoes a conformational change. (3) The third step is not entirely clear. However, it is commonly accepted that there is a specific protein (fusion receptor) on the CD4 T-cell. The fusion peptide of gp41 combines the fusion receptor to initiate the fusion of the two bilayers (Levy, 2007; Tardif and Tremblay, 2005). During the three-step process of entry of HIV into cells, the concentration of the combination of gp120 with CD4 receptor made in the first two steps has a direct and positive effect on the third step.

As the first agent to be approved in the class of fusion inhibitors, enfuvirtide functions by binding a region of the HIV envelope glycoprotein gp41 and preventing viral fusion with the target cell membrane. Enfuvirtide, and a follow-up compound involving a different amino acid sequence, T-1249, bind to one of these helical regions, preventing the hairpin folding that leads to fusion. These T-compounds are active against both CCR5- and CXCR4-using viruses, although enfuvirtide does not have substantial activity against HIV-2 (Moyle, 2003; Trottier et al., 2005).

The most common side effect, occurring in 98% of all enfuvirtide recipients, is an injection-site reaction that can generally be managed nonpharmacologically. A much less common but more significant concern is an increased risk of bacterial pneumonia (Jamjian and McNicholl, 2004). Patients treated with enfuvirtide suffered fewer of the common constitutional adverse events associated with highly active antiretroviral therapy, such as diarrhoea, nausea, fatigue, headache, insomnia and vomiting (Castagna et al., 2005). The annual cost of therapy is about US$24,000 (Jamjian and McNicholl, 2004).

Acquired resistance centres around a 10-amino-acid motif between residues 36 and 45 in gp41 that forms part of the binding site of enfuvirtide. This motif is critical for viral fusion, so enfuvirtide-resistant mutants show poor replicative capacity

* Corresponding author.
E-mail addresses: jie.lou@staff.shu.edu.cn (J. Lou), rsmith43@uottawa.ca (R.J. Smith?).

0022-5193/$ - see front matter © 2010 Elsevier Ltd. All rights reserved.
doi:10.1016/j.jtbi.2010.09.039

compared with wild type (Greenberg and Cammack, 2004). Nevertheless, a significant number of enfuvirtide-treated patients are likely to develop enfuvirtide resistance eventually (Castagna et al., 2005).

Imperfect adherence to HIV medication, due to side effects or medication fatigue, can facilitate the development of resistance (Smith, 2006). Different patterns of adherence can affect the antiretroviral response (Huang et al., 2003). Longer sequences of missed doses can increase the chance of treatment failure (Wahl and Nowak, 2000; Miron and Smith?, 2010). Thus, it is important to understand the effects of adherence, especially as enfuvirtide may be taken as monotherapy in treatment-experienced patients (Clotet et al., 2004). Since enfuvirtide is new and long-term data are not available, it will be some time before the effects of adherence can be fully delineated. Mathematical models can thus provide a potential glimpse of the effects of partial adherence to this new drug.

A handful of mathematical models have investigated the dynamics of enfuvirtide. A Markov model developed to predict the outcome of patients receiving either enfuvirtide plus optimised background (OB) or OB alone predicted that the favourable virological and immunological response to enfuvirtide plus OB could extend overall survival on average by 1.6 years compared with OB alone (6.2 vs. 4.6 years) (Fätkenheuer et al., 2004). A model of the pharmacokinetics of enfuvirtide revealed that steady-state values of peak and trough concentrations, as well as the area under the concentration–time curve, varied nearly linearly with dosage over a broad range of dosages and for different dosing regimens (Mohanty and Dixit, 2008). A model of the immuno-pathogenesis of HIV-1 infection, incorporating the effect of fusion/entry inhibitors, reverse transcriptase inhibitors and protease inhibitors, showed that combinations of two drugs which included protease inhibitors or fusion inhibitors were stronger than two-drug combinations which included reverse transcriptase inhibitors (Magombedze et al., 2008).

Impulsive differential equations have recently been used to describe the effects of adherence to antiretroviral HIV drugs (Krakovska and Wahl, 2007; Liu and Li, 2010; Liu et al., 2008; Yadav and Balakrishnan, 2006). Our previous work using impulsive differential equations has elucidated insights into preferred dosing periods and dosages (Smith and Wahl, 2004; Smith? and Aggarwala, 2009), determined regions where resistance is likely to occur (Smith and Wahl, 2005) and examined the effects of maximal allowable drug holidays (Miron and Smith?, 2010; Smith, 2006).

Here, we describe the interaction of the HIV virus with $CD4^+$ T cells in order to describe the fusion process. We determine analytical thresholds for the dosage and dosing intervals to ensure the disease-free equilibrium remains stable. We also explore the effects of partial adherence. In common with our earlier work, we consider impulsive drug dynamics independently of the non-impulsive part and use the solution to estimate dosing intervals and dosages. However, our model here incorporates drug dynamics into the model in a new way and also considers a significantly more detailed understanding of the process of attachment and infection of $CD4^+$ T cells.

This paper is organised as follows. In Section 2, we develop the mathematical model. In Section 3, we examine the model in the absence of drugs. In Section 4, we analyse the model when drugs are included. In Section 5, we illustrate the results with numerical simulations and examine the effects of partial adherence. Finally, in Section 6, we discuss the implications of the results.

2. The model

Let G_1 denote the concentration of gp120 *in vivo*, C_{D4} denote the concentration of $CD4^+$ receptor, and C_1 denote the concentration of the combination of gp120 and CD4 receptor. Let G_2 be the concentration of gp41, F_T be the concentration of the fusion protein on $CD4^+$ cells, and C_2 be the concentration of the combination of gp41 and the fusion protein. Also, let I denote the concentration of infected $CD4^+$ T cells, V denote the concentration of HIV virus and R denote the concentration of fusion inhibitor enfuvirtide. Then we have the following system:

$$\begin{aligned}
\frac{dG_1}{dt} &= bV-\mu_G G_1-\beta_1 G_1 C_{D4},\\
\frac{dC_{D4}}{dt} &= ps_T-\mu_T C_{D4}-\beta_1 G_1 C_{D4},\\
\frac{dC_1}{dt} &= \beta_1 G_1 C_{D4}-d_1 C_1,\\
\frac{dG_2}{dt} &= aC_1-\mu_G G_2-\beta_2\left(\frac{IC_{50}}{IC_{50}+R}\right)G_2 F_T,\\
\frac{dF_T}{dt} &= qs_T-\mu_T F_T-\beta_2\left(\frac{IC_{50}}{IC_{50}+R}\right)G_2 F_T,\\
\frac{dC_2}{dt} &= \beta_2\left(\frac{IC_{50}}{IC_{50}+R}\right)G_2 F_T-d_2 C_2,\\
\frac{dI}{dt} &= kC_2-d_I I,\\
\frac{dV}{dt} &= nd_I I-\mu_V V,\\
\frac{dR}{dt} &= -gR,
\end{aligned} \tag{2.1}$$

for $t \neq t_k$. The impulsive effect is described by

$$R(t_k^+) = R(t_k^-)+R^i$$

for $t=t_k$.

In this model, we describe the three steps during the entry of HIV into cells by the first three equations of system (2.1). A new generation of HIV virus will be produced if fusion of gp41 with the fusion protein F_T can be carried out successfully. That is, we assume that the $CD4^+$ T cell can be infected by HIV virus once HIV fusion is completed and progeny HIV virus will be produced thereafter.

In the first equation of system (2.1), the term bV denotes the multiplication capacity of gp120 in response to virus. In the fourth equation, aC_1 represents the successful exposure of gp41. We assume it has a positive relation with C_1, the concentration of the gp120/CD4 complex, since gp41 is exposed until attachment has finished. The parameter μ_G denotes the decay of gp120 and gp41, β_1 denotes the bonding force between gp120 and CD4 receptor, and β_2 denotes the bonding force between gp41 and fusion protein. It is likely that β_2 is a function of C_1 but, for simplicity, we have assumed it is constant. The Hill function $IC_{50}/(IC_{50}+R)$ represents the degree to which fusion inhibitors block G_2 and F_T from fusing together, which decreases the value of β_2. The parameter IC_{50} represents the concentration of drug which inhibits viral replication by 50%.

In the second and the fifth equations, s_T represents the source of susceptible $CD4^+$ T cells, p and q denote the number of CD4 receptors and the fusion protein on one $CD4^+$ T cell respectively, while μ_T represents the death rate of healthy $CD4^+$ T cells. In the third and sixth equations, d_1 denotes the dissociation rate of C_1 and d_2 the dissociation rate of C_2. In order to simplify the model, we assume that C_1 will not return to gp120 and CD4 after dissociation. Similar assumptions are made for C_2. In the eighth equation, n represents the number of virus particles that are

produced by one infected CD4$^+$ T cell. Since the ability of the virus to successfully invade a CD4$^+$ T cell depends on fusion, we assume the production of infected CD4$^+$ T cells is proportional to C_2 with rate k. The death rate of infected CD4$^+$ T cells is d_I. Parameter μ_V represents the clearance rate of HIV virus. Here, we ignore effects of the immune system except possibly as a constant effect on the clearance rate of virus.

In the seventh equation, I represents the concentration of infected CD4$^+$ T cells by HIV virus. In the ninth and tenth equations, $R(t)$ denotes the drug concentration in plasma. Parameter g represents the rate at which the drug is cleared. R^i is the dosage (a constant) that is taken at each impulse time t_k ($k=1, 2, 3\ldots$). Note that the impulse times t_k may not be fixed, since drugs may be taken at either regular or irregular intervals. However, since R^i is the concentration contained within each dose, we expect it to be constant (e.g. 4.59 μg/mL Castagna et al., 2005). The dosing times are prescribed (for example, twice a day Castagna et al., 2005), but lapses in adherence may result in variable dosing times.

The model is illustrated in Fig. 1. Parameters are listed in Table 1.

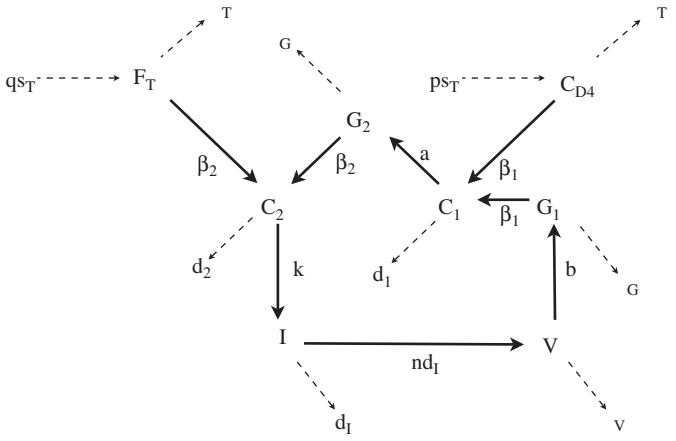

Fig. 1. The model. Here, F_T is the concentration of fusion protein on CD4 cells, G_1 is the concentration of gp120 *in vivo*, C_{D4} is the concentration of CD4 receptors, C_1 is the concentration of the combination of gp120 and the CD4 receptor, G_2 is the concentration of gp41, C_2 is the concentration of the combination of gp41 and the fusion protein, I are infected cells and V is the virus. The effects of enfuvirtide are to reduce β_2 and hence the formation of C_2.

3. The system without drugs

When $R=0$, the model becomes

$$\frac{dG_1}{dt} = bV-\mu_G G_1-\beta_1 G_1 C_{D4},$$

$$\frac{dC_{D4}}{dt} = ps_T-\mu_T C_{D4}-\beta_1 G_1 C_{D4},$$

$$\frac{dC_1}{dt} = \beta_1 G_1 C_{D4}-d_1 C_1,$$

$$\frac{dG_2}{dt} = aC_1-\mu_G G_2-\beta_2 G_2 F_T,$$

$$\frac{dF_T}{dt} = qs_T-\mu_T F_T-\beta_2 G_2 F_T,$$

$$\frac{dC_2}{dt} = \beta_2 G_2 F_T-d_2 C_2,$$

$$\frac{dI}{dt} = kC_2-d_I I,$$

$$\frac{dV}{dt} = nd_I I-\mu_V V. \tag{3.2}$$

Table 1
Parameters.

Parameter	Definition	Value	Units	Reference
G_1	gp120 molecule population	Variable	mm^{-3}	–
C_{D4}	CD4* receptor population	Variable	mm^{-3}	–
C_1	Combination of gp120 molecule and CD4 receptor population	Variable	mm^{-3}	–
G_2	gp41 protein population	Variable	mm^{-3}	–
F_T	Fusion protein (on CD4$^+$ cells) population	Variable	mm^{-3}	–
C_2	Combination of gp41 and the fusion protein population	Variable	mm^{-3}	–
V	Virus	Variable	mm^{-3}	–
I	Infected CD4$^+$ cells	Variable	mm^{-3}	–
R	Drug	Variable	μg mm^{-3}	–
b	Multiplication capacity of gp120 and gp41	42	day^{-1}	Estimate
β_1	Bonding force between gp120 and CD4 receptor per concentration of each molecule in complex	10^{-5}	mm^3 day^{-1}	Perelson et al. (1993)
β_2	Bonding force between gp41 and F_T per concentration of each molecule in complex	10^{-5}	mm^3 day^{-1}	Perelson et al. (1993)
μ_T	Death rate of CD4 receptor	0.05	day^{-1}	Perelson et al. (1993)
a	Exposure rate of gp41	25	day^{-1}	Estimate
d_1	Dissociation rate of C_1	0.4	day^{-1}	Estimate
p	Number of CD4 receptors on one CD4$^+$ T cell	1	cell^{-1}	He (2006)
q	Number of fusion receptors on one CD4$^+$ T cell	0.5	cell^{-1}	Levy (2007)
k	Infection rate of CD4$^+$ T cells	0.6	day^{-1}	Estimate
s_T	Source rate of susceptible CD4$^+$ T cells	80	day^{-1} mm^{-3}	Perelson et al. (1993), Smith and Wahl (2005)
μ_G	Death rate of gp120 and gp41	5	day^{-1}	Perelson et al. (1993), Smith and Wahl (2005)
IC_{50}	Concentration of drug which inhibits viral replication by 50%	10^{-5}	μg mm^{-3}	Wahl and Nowak (2000)
g	Rate that the drug is cleared *in vivo*	1	day^{-1}	Smith and Wahl (2005)
n	Rate of production of virions per infected cell	540		Tsai et al. (2007)
μ_V	Clearance rate of infectious virus	3	day^{-1}	Smith? and Aggarwala (2009)
d_I	Death rate of infected T cells	0.5	day^{-1}	Perelson et al. (1993), Smith and Wahl (2005)
d_2	Dissociation rate of C_2	0.4	day^{-1}	Estimate

First, we analyse the model in the absence of treatment. In this section, we discuss the existence of the equilibria and their stability.

3.1. The disease-free equilibrium

The disease-free equilibrium always exists and is in the form

$$E^0(G_1^0,C_{D4}^0,C_1^0,G_2^0,F_T^0,C_2^0,I^0,V^0)=\left(0,\frac{ps_T}{\mu_T},0,0,\frac{qs_T}{\mu_T},0,0,0\right).$$

The linearisation of the first, third, fourth, sixth, seventh and eighth equations of model (3.2) at the disease-free state E^0 can be rewritten in the following form:

$$\frac{dX}{dt}=(Y_{E^0}-Z_{E^0})X,$$

where

$$X=[G_1,\ C_1,\ G_2,\ C_2,\ I,\ V]^T,$$

$$Y_{E^0}=\begin{bmatrix}0&0&0&0&0&b\\ \beta_1C_{D4}^0&0&0&0&0&0\\ 0&a&0&0&0&0\\ 0&0&\beta_2F_T^0&0&0&0\\ 0&0&0&k&0&0\\ 0&0&0&0&nd_I&0\end{bmatrix},$$

$$Z_{E^0}=\begin{bmatrix}\mu_G+\beta_1C_{D4}^0&0&0&0&0&0\\ 0&d_1&0&0&0&0\\ 0&0&\mu_G+\beta_2F_T^0&0&0&0\\ 0&0&0&d_2&0&0\\ 0&0&0&0&d_I&0\\ 0&0&0&0&0&\mu_V\end{bmatrix}.$$

A threshold criteria, R_0, can be derived using the spectral radius of the next-generation matrix (Heffernan et al., 2005; van den Driessche and Watmough, 2002). Therefore, to find R_0, we must find the largest eigenvalue of $Y_{E^0}Z_{E^0}^{-1}$. Thus,

$$R_0=\rho(Y_{E_0}Z_{E_0}^{-1})=\max_{|\lambda|}\det\begin{bmatrix}\lambda&0&0&0&0&-\frac{b}{\mu_V}\\ -\frac{\beta_1C_{D4}^0}{\mu_G+\beta_1C_{D4}^0}&\lambda&0&0&0&0\\ 0&-\frac{a}{d_1}&\lambda&0&0&0\\ 0&0&-\frac{\beta_2F_T^0}{\mu_G+\beta_2F_T^0}&\lambda&0&0\\ 0&0&0&-\frac{k}{d_2}&\lambda&0\\ 0&0&0&0&-n&\lambda\end{bmatrix}.$$

Then the characteristic equation of $Y_{E_0}Z_{E_0}^{-1}$ is

$$\lambda^6-ABCDEF=0,$$

where

$$A=\frac{b}{\mu_V},\quad B=\frac{\beta_1C_{D4}^0}{\mu_G+\beta_1C_{D4}^0},\quad C=\frac{a}{d_1},\quad D=\frac{\beta_2F_T^0}{\mu_G+\beta_2F_T^0},$$
$$E=\frac{k}{d_2},\quad F=n.$$

Then

$$R_0=(ABCDEF)^{1/6}=\left(\frac{abknpq\beta_1\beta_2s_T^2}{d_1d_2\mu_V(ps_T\beta_1+\mu_G\mu_T)(qs_T\beta_2+\mu_G\mu_T)}\right)^{1/6}.$$

Thus, E^0 always exists, is locally stable if $R_0<1$ and unstable if $R_0>1$ (van den Driessche and Watmough, 2002).

We use the threshold, R_0, to answer the question of whether the infection can be established. When $R_0>1$, HIV infection can take hold. Otherwise, the virus will be eliminated.

3.2. The endemic equilibrium

The endemic equilibrium (if it exists) should be in form $E^*(G_1^*, C_{D4}^*, C_1^*, G_2^*, F_T^*, C_2^*, I^*, V^*)$, in which

$$C_{D4}^*=\frac{ps_T}{\beta_1G_1^*+\mu_T},$$

$$C_1^*=\frac{\beta_1G_1^*C_{D4}^*}{d_1}=\frac{ps_T\beta_1G_1^*}{d_1(\beta_1G_1^*+\mu_T)},$$

$$V^*=\frac{(\mu_G+\beta_1C_{D4}^*)}{b}G_1^*=\frac{(ps_T\beta_1+\mu_G\beta_1G_1^*+\mu_G\mu_T)G_1^*}{b(\beta_1G_1^*+\mu_T)},$$

$$I^*=\frac{\mu_VV^*}{nd_I}=\frac{\mu_V(ps_T\beta_1+\mu_G\beta_1G_1^*+\mu_G\mu_T)G_1^*}{bd_In(\beta_1G_1^*+\mu_T)},$$

$$C_2^*=\frac{d_II^*}{k}=\frac{\mu_V(ps_T\beta_1+\mu_G\beta_1G_1^*+\mu_G\mu_T)G_1^*}{bkn(\beta_1G_1^*+\mu_T)},$$

$$G_2^*=\left(\frac{abknps_T\beta_1-d_1d_2\mu_V[ps_T\beta_1+\mu_G(\beta_1G_1^*+\mu_T)]}{bd_1kn\mu_G(\beta_1G_1^*+\mu_T)}\right)G_1^*,$$

$$F_T^*=\frac{d_2C_2^*}{\beta_2G_2^*}=\frac{d_2d_1\mu_G\mu_V(ps_T\beta_1+\mu_G\beta_1G_1^*+\mu_G\mu_T)G_1^*}{\beta_2(abknps_T\beta_1-d_1d_2\mu_V[ps_T\beta_1+\mu_G(\beta_1G_1^*+\mu_T)])}.$$

G_1^* (if it exists) is a positive, real root of the cubic equation

$$\phi(G_1)=\Theta_1G_1^3+\Theta_2G_1^2+\Theta_3G_1+\Theta_4=0,$$

where

$$\Theta_1=d_1d_2^2\beta_1^2\beta_2\mu_G^2\mu_V^2,$$

$$\Theta_2=-d_2\beta_1\mu_G\mu_V(abknps_T\beta_1\beta_2+bd_1knqs_T\beta_1\beta_2+bd_1kn\beta_1\mu_G\mu_T-2d_1d_2ps_T\beta_1\beta_2\mu_V-2d_1d_2\beta_2\mu_G\mu_T\mu_V),$$

$$\Theta_3=ab^2k^2n^2pqs_T^2\beta_1^2\beta_2+d_1d_2^2\beta_2(ps_T\beta_1+\mu_G\mu_T)^2\mu_V^2-bd_2kn\beta_1\mu_V(ap^2s_T^2\beta_1\beta_2+d_1pqs_T^2\beta_1\beta_2+d_1ps_T\beta_1\mu_G\mu_T+aps_T\beta_2\mu_G\mu_T+2d_1qs_T\beta_2\mu_G\mu_T+2d_1\mu_G^2\mu_T^2),$$

$$\Theta_4=bkn\mu_T(abknpqs_T^2\beta_1\beta_2-d_1d_2pqs_T^2\beta_1\beta_2\mu_V-d_1d_2ps_T\beta_1\mu_G\mu_T\mu_V-d_1d_2qs_T\beta_2\mu_G\mu_T\mu_V-d_1d_2\mu_G^2\mu_T^2\mu_V).$$

Then, for the existence of positive endemic equilibrium E^*, we have the following.

Theorem 3.1. *When $R_0>1$, one and only one endemic equilibrium E^* exists. Otherwise, E^* does not exist.*

Proof. For the existence of G_2^*, we need $0<G_1^*<\tilde{G}_1$, where

$$\tilde{G}_1=\frac{abknps_T\beta_1-ps_T\beta_1d_1d_2\mu_V-d_1d_2\mu_G\mu_T\mu_V}{d_1d_2\beta_1\mu_G\mu_V}.$$

So, for $\tilde{G}_1>0$, we need

$$abknps_T\beta_1>d_1d_2\mu_V(ps_T\beta_1+\mu_G\mu_T). \tag{3.3}$$

Otherwise, $\tilde{G}_1 < 0$ and no positive endemic equilibrium exists. Under condition (3.3), we also have that

$$\phi(\tilde{G}_1) = \frac{ab^2k^2n^2p^2s_T^2\beta_1^2\mu_T(d_1d_2\mu_V - abkn)}{d_1d_2\mu_V} < 0.$$

1. When $R_0 > 1$, we have $\Theta_4 > 0$ and $\tilde{G}_1 > 0$ (since (3.3) is satisfied). So $\phi(G_1) = 0$ can have at most two positive roots. Since $\phi(\tilde{G}_1) < 0$, so $\phi(G_1) = 0$ can have just two positive roots and only the smaller root of $\phi(G_1) = 0$ lies in the range $0 < G_1 < \tilde{G}_1$. That is, the smaller root satisfies $G_2^* > 0$, while the larger root has the property that $G_2^* < 0$. Hence, when $R_0 > 1$, there is only one biologically meaningful endemic equilibrium.
2. When $R_0 \le 1$, we have $\Theta_4 \le 0$.
   (a) When (3.3) cannot be satisfied, $\tilde{G}_1$ is negative and no positive endemic equilibrium exists.
   (b) When (3.3) is satisfied, we rewrite Θ_3 and can get

$$\begin{aligned}\Theta_3 = {} & bkn\beta_1(abknpqs_T^2\beta_1\beta_2 - d_1d_2pqs_T^2\beta_1\beta_2\mu_V \\ & - d_1d_2ps_T\beta_1\mu_G\mu_T\mu_V - d_1d_2qs_T\beta_2\mu_G\mu_T\mu_V - d_1d_2\mu_G^2\mu_T^2\mu_V) \\ & - bd_1d_2kn\beta_1\mu_G\mu_T(qs_T\beta_2 + \mu_G\mu_T)\mu_V \\ & - d_2\beta_2\mu_V(ps_T\beta_1 + \mu_G\mu_T)(abknps_T\beta_1 \\ & - d_1d_2ps_T\beta_1\mu_V - d_1d_2\mu_G\mu_T\mu_V), \\ < {} & 0.\end{aligned}$$

   Then the derivative function of $\phi(G_1)$

$$\Psi(G_1) \equiv 3\Theta_1G_1^2 + 2\Theta_2G_1 + \Theta_3 = 0$$

   has two real roots: one is positive and the other is negative since $\Theta_1 > 0$ and $\Theta_3 < 0$. This means $\phi(G_1) = 0$ can have one and only one positive root, which is denoted by $\hat{G}_1$. Also since $\phi(\tilde{G}_1) < 0$, $\tilde{G}_1 < \hat{G}_1$. That means $\phi(G_1) = 0$ does not have a positive root that satisfies $G_1^* < \tilde{G}_1$. Hence, when $R_0 \le 1$, there is no endemic equilibrium.

This completes the proof. □

3.3. The global stability of E_0

Theorem 3.2. *When $R_0 \le 1$, the disease-free equilibrium E_0 is globally asymptotically stable and it is the unique equilibrium. Otherwise, E_0 is unstable and a unique endemic equilibrium E^* exists.*

Proof. In the absence of HIV, the concentration of the $CD4^+$ receptor, C_{D4}, and the concentration of the fusion protein on $CD4^+$ cells, F_T, should satisfy

$$\frac{dC_{D4}}{dt} = ps_T - \mu_T C_{D4},$$

$$\frac{dF_T}{dt} = qs_T - \mu_T F_T. \tag{3.4}$$

For example, the solution of the first equation of system (3.4) is

$$C_{D4}(t) = \frac{ps_T}{\mu_T} - \left(\frac{ps_T}{\mu_T} - C_{D4}(0)\right)e^{-\mu_T t}.$$

It follows that $C_{D4}(t) \to ps_T/\mu_T$ when $t \to \infty$. If the initial value satisfies $C_{D4}(0) < ps_T/\mu_T$, then all trajectories remain below ps_T/μ_T. Conversely, if the initial value satisfies $C_{D4}(0) > ps_T/\mu_T$, then all trajectories remain above ps_T/μ_T.

Suppose our initial values of the immune system are at or below its steady state. Then the inequalities $C_{D4} \le ps_T/\mu_T$ and $F_T \le qs_T/\mu_T$ can be used in our proof below. To prove the global stability of the disease-free equilibrium, we take a Liapunov function of the form:

$$L_V = \mathcal{M}G_1 + \mathcal{N}C_1 + \mathcal{X}G_2 + \mathcal{Y}C_2 + \mathcal{P}I + \mathcal{Q}V,$$

where constants $\mathcal{M} > 0$, $\mathcal{N} > 0$, $\mathcal{X} > 0$, $\mathcal{Y} > 0$, $\mathcal{P} > 0$ and $\mathcal{Q} > 0$. Then the derivative of L_V along the solutions of (3.2) is

$$\begin{aligned}\frac{d(L_V)}{dt} = {} & (b\mathcal{M} - \mu_V\mathcal{Q})V + (nd_I\mathcal{Q} - d_I\mathcal{P})I + (a\mathcal{X} - \mathcal{N}d_1)C_1 + (k\mathcal{P} - d_2\mathcal{Y})C_2 \\ & + \beta_1(\mathcal{N} - \mathcal{M})G_1C_{D4} + \beta_2(\mathcal{Y} - \mathcal{X})G_2F_T - \mu_G\mathcal{M}G_1 - \mu_G\mathcal{X}G_2 \\ \le {} & (b\mathcal{M} - \mu_V\mathcal{Q})V + (nd_I\mathcal{Q} - d_I\mathcal{P})I + (a\mathcal{X} - \mathcal{N}d_1)C_1 + (k\mathcal{P} - d_2\mathcal{Y})C_2 \\ & + \left[\beta_1(\mathcal{N} - \mathcal{M})\frac{ps_T}{\mu_T} - \mu_G\mathcal{M}\right]G_1 + \left[\beta_2(\mathcal{Y} - \mathcal{X})\frac{qs_T}{\mu_T} - \mu_G\mathcal{X}\right]G_2.\end{aligned}$$

Thus, we can choose proper positive numbers $\mathcal{M}, \mathcal{N}, \mathcal{X}, \mathcal{Y}, \mathcal{P}$ and $\mathcal{Q}$ as follows:

$$\mathcal{M} = \frac{\mu_V}{bn}, \quad \mathcal{N} = \frac{\mu_V(ps_T\beta_1 + \mu_G\mu_T)}{bnps_T\beta_1}, \quad \mathcal{X} = \frac{d_1\mu_V(ps_T\beta_1 + \mu_G\mu_T)}{abnps_T\beta_1},$$

$$\mathcal{P} = 1, \quad \mathcal{Q} = \frac{1}{n}, \quad \mathcal{Y} = \frac{d_1\mu_V(ps_T\beta_1 + \mu_G\mu_T)(qs_T\beta_2 + \mu_G\mu_T)}{abnpqs_T^2\beta_1\beta_2}.$$

Hence

$$\begin{aligned}\frac{d(L_V)}{dt} & \le (k\mathcal{P} - d_2\mathcal{Y})C_2 \\ & = \left(k - \frac{d_1d_2\mu_V(ps_T\beta_1 + \mu_G\mu_T)(qs_T\beta_2 + \mu_G\mu_T)}{abnpqs_T^2\beta_1\beta_2}\right)C_2 \\ & = \frac{k}{R_0^6}(R_0^6 - 1)C_2.\end{aligned}$$

Then we have $d(L_V)/dt \le 0$ when $R_0 \le 1$, and $d(L_V)/dt = 0$ implies $C_2 = 0$. When $C_2 = 0$, from system (3.2) we get that $I \to 0$, $V \to 0, G_1 \to 0, C_1 \to 0, G_2 \to 0$ respectively when $t \to \infty$. Then the disease-free equilibrium is globally asymptotically stable when $R_0 \le 1$ by the Liapunov–Lasalle theorem (Hethcote, 2000). This completes the proof. □

Remark. Although E^* exists for $R_0 > 1$, we have not proven that it is locally stable. However, numerical simulations converged to this equilibrium and did not reveal any other phenomena.

4. The system with drugs

There is an impulsive periodic orbit R^* satisfying the equations

$$\frac{dR}{dt} = -gR, \quad t \ne t_k,$$

$$\Delta R = R^i, \quad t = t_k$$

if the time between doses is constant, i.e., $\tau \equiv t_{k+1} - t_k$.

This impulsive periodic orbit satisfies

$$\frac{R^i e^{-g\tau}}{1 - e^{-g\tau}} \le R^* \le \frac{R^i}{1 - e^{-g\tau}}. \tag{4.5}$$

Note that this orbit requires the impulse times to be fixed (see Miron and Smith?, 2010).

The disease-free orbit is in the form

$$\tilde{E}^0(G_1^0, C_{D4}^0, C_1^0, G_2^0, F_T^0, C_2^0, I^0, V^0, R^*) = \left(0, \frac{ps_T}{\mu_T}, 0, 0, \frac{qs_T}{\mu_T}, 0, 0, 0, R^*\right).$$

Note that R^* is nonconstant, but that other values are all constants.

The only differences between systems (2.1) and (3.2) are that terms β_2 in system (3.2) are substituted for the term $\beta_2(IC_{50}/(IC_{50} + R))$ in system (2.1).

The corresponding Jacobian matrix does not include the R equation, but other terms contain R^*, which is not constant. Thus, there are no equilibria in the impulsive system, but rather equilibria-like orbits. However, since the system is autonomous and R^* is bounded, the stability of the equilibria-like orbits can be calculated using the eigenvalues of Jacobian matrix. See Smith? and Aggarwala (2009) for more discussions.

Thus, similar to Section 3.1, the threshold for system (2.1) is

$$\tilde{R}_0=\left(\frac{abknpqIC_{50}\beta_1\beta_2 s_T^2}{d_1d_2\mu_V(ps_T\beta_1+\mu_G\mu_T)(qs_T\beta_2IC_{50}+(IC_{50}+R^*)\mu_G\mu_T)}\right)^{1/6}. \tag{4.6}$$

The endemic periodic orbit is in the form $\tilde{E}^*(\tilde{G}_1^*,\tilde{C}_{D4}^*,\tilde{C}_1^*,\tilde{G}_2^*,\tilde{F}_T^*,\tilde{C}_2^*,\tilde{I}^*,\tilde{V}^*,R^*)$ where

$$\tilde{C}_{D4}^*=\frac{ps_T}{\beta_1\tilde{G}_1^*+\mu_T},$$

$$\tilde{C}_1^*=\frac{\beta_1\tilde{G}_1^*\tilde{C}_{D4}^*}{d_1}=\frac{ps_T\beta_1\tilde{G}_1^*}{d_1(\beta_1\tilde{G}_1^*+\mu_T)},$$

$$\tilde{V}^*=\frac{(\mu_G+\beta_1\tilde{C}_{D4}^*)}{b}\tilde{G}_1^*=\frac{(ps_T\beta_1+\mu_G\beta_1\tilde{G}_1^*+\mu_G\mu_T)\tilde{G}_1^*}{b(\beta_1\tilde{G}_1^*+\mu_T)},$$

$$\tilde{I}^*=\frac{\mu_V\tilde{V}^*}{nd_I}=\frac{\mu_V(ps_T\beta_1+\mu_G\beta_1\tilde{G}_1^*+\mu_G\mu_T)\tilde{G}_1^*}{bd_In(\beta_1\tilde{G}_1^*+\mu_T)},$$

$$\tilde{C}_2^*=\frac{d_I\tilde{I}^*}{k}=\frac{\mu_V(ps_T\beta_1+\mu_G\beta_1\tilde{G}_1^*+\mu_G\mu_T)\tilde{G}_1^*}{bkn(\beta_1\tilde{G}_1^*+\mu_T)},$$

$$\tilde{G}_2^*=\left(\frac{abknps_T\beta_1-d_1d_2\mu_V[ps_T\beta_1+\mu_G(\beta_1\tilde{G}_1^*+\mu_T)]}{bd_1kn\mu_G(\beta_1\tilde{G}_1^*+\mu_T)}\right)\tilde{G}_1^*,$$

$$\tilde{F}_T^*=\frac{d_2(IC_{50}+R^*)\tilde{C}_2^*}{IC_{50}\beta_2\tilde{G}_2^*}=\frac{d_2d_1\mu_G\mu_V(IC_{50}+R^*)(ps_T\beta_1+\mu_G\beta_1\tilde{G}_1^*+\mu_G\mu_T)\tilde{G}_1^*}{IC_{50}\beta_2(abknps_T\beta_1-d_1d_2\mu_V[ps_T\beta_1+\mu_G(\beta_1\tilde{G}_1^*+\mu_T)])}.$$

$\tilde{G}_1^*$ (if it exists) is a positive, real root of the cubic equation

$$\phi(\tilde{G}_1)=\tilde{\Theta}_1\tilde{G}_1^3+\tilde{\Theta}_2\tilde{G}_1^2+\tilde{\Theta}_3\tilde{G}_1+\tilde{\Theta}_4=0,$$

where

$$\tilde{\Theta}_1=d_1d_2^2\beta_1^2\beta_2\left(\frac{IC_{50}}{IC_{50}+R^*}\right)\mu_G^2\mu_V^2,$$

$$\begin{aligned}\tilde{\Theta}_2=&-d_2\beta_1\mu_G\mu_V(abknps_T\beta_1\beta_2\left(\frac{IC_{50}}{IC_{50}+R^*}\right)\\&+bd_1knqs_T\beta_1\beta_2\left(\frac{IC_{50}}{IC_{50}+R^*}\right)\\&+bd_1kn\beta_1\mu_G\mu_T-2d_1d_2ps_T\beta_1\beta_2\left(\frac{IC_{50}}{IC_{50}+R^*}\right)\mu_V\\&-2d_1d_2\beta_2\left(\frac{IC_{50}}{IC_{50}+R^*}\right)\mu_G\mu_T\mu_V),\end{aligned}$$

$$\begin{aligned}\tilde{\Theta}_3=&ab^2k^2n^2pqs_T^2\beta_1^2\beta_2\left(\frac{IC_{50}}{IC_{50}+R^*}\right)\\&+d_1d_2^2\beta_2\left(\frac{IC_{50}}{IC_{50}+R^*}\right)(ps_T\beta_1+\mu_G\mu_T)^2\mu_V^2\\&-bd_2kn\beta_1\mu_V(ap^2s_T^2\beta_1\beta_2\left(\frac{IC_{50}}{IC_{50}+R^*}\right)\\&+d_1pqs_T^2\beta_1\beta_2\left(\frac{IC_{50}}{IC_{50}+R^*}\right)\\&+d_1ps_T\beta_1\mu_G\mu_T+aps_T\beta_2\left(\frac{IC_{50}}{IC_{50}+R^*}\right)\mu_G\mu_T\\&+2d_1qs_T\beta_2\left(\frac{IC_{50}}{IC_{50}+R^*}\right)\mu_G\mu_T+2d_1\mu_G^2\mu_T^2),\end{aligned}$$

$$\begin{aligned}\tilde{\Theta}_4=&bkn\mu_T(abknpqs_T^2\beta_1\beta_2\left(\frac{IC_{50}}{IC_{50}+R^*}\right)\\&-d_1d_2pqs_T^2\beta_1\beta_2\left(\frac{IC_{50}}{IC_{50}+R^*}\right)\mu_V\\&-d_1d_2ps_T\beta_1\mu_G\mu_T\mu_V-d_1d_2qs_T\beta_2\left(\frac{IC_{50}}{IC_{50}+R^*}\right)\mu_G\mu_T\mu_V\\&-d_1d_2\mu_G^2\mu_T^2\mu_V).\end{aligned}$$

Obviously, $\tilde{R}_0>1$ is equivalent to $\tilde{\Theta}_4>0$.

Thus, using similar methods as Section 3.3, we have the following theorem about the existence and stability of the disease-free periodic orbit and the endemic periodic orbit.

Theorem 4.1. *Let $\tilde{R}_0$ be as in (4.6). The disease-free periodic orbit $\tilde{E}_0$ always exists. When $\tilde{R}_0<1$, $\tilde{E}_0$ is globally stable and the endemic periodic orbit $\tilde{E}^*$ does not exist. When $\tilde{R}_0>1$, $\tilde{E}_0$ is unstable and $\tilde{E}^*$ exists.*

Remarks. 1. Although $\tilde{E}^*$ exists when $\tilde{R}_0>1$, it may or may not be stable, depending on parameters. If it is unstable, then we may have higher-order behaviour, such as higher-order periodicity or chaos.

2. Note that, since $\tilde{R}_0$ is fluctuating due to the impulsive effect, we require $\tilde{R}_0<1$ to hold at all times for eradication to be guaranteed. Conversely, the theorem only guarantees existence of $\tilde{E}^*$ and instability of $\tilde{E}_0$ when $\tilde{R}_0>1$ for all times. If $\tilde{R}_0$ fluctuates around 1, then the results are indeterminate.

We now examine the dependence upon the dosage and dosing interval. As $R^*\to\infty$, $\tilde{R}_0\to 0$ and the endemic periodic orbit ceases to exist.

Define

$$R_1=\frac{M}{\Psi},\quad R_2=\frac{M}{\Phi},\quad \tau_1=\frac{1}{g}\ln\left(1+\frac{R^i}{M}\right)\quad\text{and}\quad \tau_2=-\frac{1}{g}\ln\left(1-\frac{R^i}{M}\right),$$

where $\Psi=e^{-g\tau}/(1-e^{-g\tau}),\Phi=1/(1-e^{-g\tau})$ and

$$\begin{aligned}M=&IC_{50}\left(-1+qs_T\beta_2\left(-\frac{1}{\mu_G\mu_T}+\frac{abknps_T\beta_1}{d_1d_2\mu_G\mu_T\mu_V(ps_T\beta_1+\mu_G\mu_T)}\right)\right)\\=&\frac{IC_{50}(abknpqs_T^2\beta_1\beta_2-d_1d_2\mu_V(ps_T\beta_1+\mu_G\mu_T)(qs_T\beta_2+\mu_G\mu_T))}{d_1d_2\mu_G\mu_T\mu_V(ps_T\beta_1+\mu_G\mu_T)}.\end{aligned}$$

Theorem 4.2. *When $R^i>R_1$, $\tilde{E}_0$ is globally stable and $\tilde{E}^*$ does not exist. When the dosage satisfies $0\le R^i<R_2$, $\tilde{E}_0$ is unstable and $\tilde{E}^*$ exists.*

Proof. From (4.5), we have $R^i\Psi\le R^*\le R^i\Phi$.

If $R^i>R_1$, then

$$R^i>\frac{M(1-e^{-g\tau})}{e^{-g\tau}}$$

$$\frac{e^{-g\tau}R^i}{1-e^{-g\tau}}>M$$

$$\Rightarrow\quad M<R^*.$$

Thus,

$$\begin{aligned}&IC_{50}[abknpqs_T^2\beta_1\beta_2-d_1d_2\mu_V(ps_T\beta_1+\mu_G\mu_T)(qs_T\beta_2+\mu_G\mu_T)]\\&\quad<R^*d_1d_2\mu_G\mu_T\mu_V(ps_T\beta_1+\mu_G\mu_T)\\&IC_{50}abknpqs_T^2\beta_1\beta_2<d_1d_2\mu_V(ps_T\beta_1+\mu_G\mu_T)(qs_T\beta_2IC_{50}\\&\quad+\mu_G\mu_TIC_{50}+\mu_G\mu_TR^*)\\&\tilde{R}_0<1.\end{aligned}$$

It follows from Theorem 4.1 that $\tilde{E}_0$ is globally stable and $\tilde{E}^*$ does not exist.

If $R^i < R_2$, then

$$R^i < \frac{IC_{50}}{d_1 d_2 \mu_G \mu_T \mu_V (ps_T\beta_1 + \mu_G\mu_T)\Phi}[abknpqs_T^2\beta_1\beta_2 - d_1 d_2 \mu_V (ps_T\beta_1 + \mu_G\mu_T)(qs_T\beta_2 + \mu_G\mu_T)]$$

$$d_1 d_2 \mu_G \mu_T \mu_V (ps_T\beta_1 + \mu_G\mu_T)R^i\Phi < IC_{50}[abknpqs_T^2\beta_1\beta_2 - d_1 d_2 \mu_V (ps_T\beta_1 + \mu_G\mu_T)(qs_T\beta_2 + \mu_G\mu_T)]$$

$$IC_{50}abknpqs_T^2\beta_1\beta_2 > d_1 d_2 \mu_G \mu_T \mu_V (ps_T\beta_1 + \mu_G\mu_T)R^i\Phi + IC_{50}d_1 d_2 \mu_V (ps_T\beta_1 + \mu_G\mu_T)(qs_T\beta_2 + \mu_G\mu_T)$$
$$\geq d_1 d_2 \mu_G \mu_T \mu_V (ps_T\beta_1 + \mu_G\mu_T)R^* + IC_{50}d_1 d_2 \mu_V (ps_T\beta_1 + \mu_G\mu_T)(qs_T\beta_2 + \mu_G\mu_T)$$

$$\therefore \quad \tilde{R}_0 > 1.$$

It follows from Theorem 4.1 that $\tilde{E}_0$ is unstable and $\tilde{E}^*$ exists. □

Remark. Equivalently, for fixed dosage, the disease-free periodic orbit will be stable if $0 \leq \tau < \tau_1$ and unstable if $\tau > \tau_2$. It follows that, if the drug is taken sufficiently often, then the disease can be theoretically controlled. See Fig. 2.

5. Numerical simulations

We define two therapy strategies:

1. Perfect adherence: drugs are given at fixed intervals τ.
2. Partial adherence: drugs are given at fixed intervals τ, except for a series of "drug holidays", where therapy is halted for a finite amount of time.

Parameters are listed in Table 1. Parameter n is composed of two factors: one is the probability that HIV virus is infectious; the other is the rate of production of virions per infected cell. We choose $n = 0.1 \times 5400 = 540$ (Tsai et al., 2007), where 0.102 is the rate of infectious virus in total HIV virus offspring. According to Zhu et al. (2006), every HIV virus has average 42 (i.e. 3 molecules per trimer × 14 trimers) gp120 receptors. Note that the values of parameters β_1 and β_2 are estimated from the infection rate of healthy $CD4^+$ T cells by HIV virus (Perelson et al., 1993). We assume there are, on average, 800/ml^3 $CD4^+$ T lymphocytes in a healthy individual. The initial conditions were $G_1(0)=2100$ (i.e. 50×42), $C_{D4}(0)=800$, $C_1(0)=0$, $G_2(0)=1050$ (i.e. $50 \times 42 \times 0.5$),$F_T(0)=800$,$C_2(0)=0$,$I(0)=0$ and $V(0)=50$. The unit of each concentration is mm^{-3}.

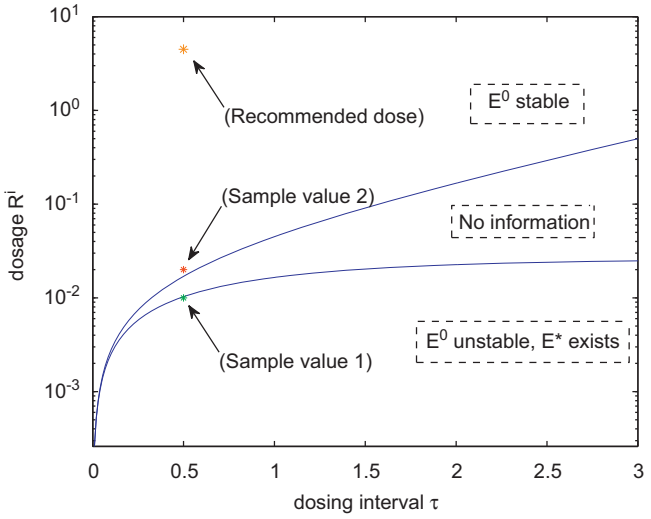

Fig. 2. Regions of stability. If R^i is sufficiently large or τ sufficiently small, then E_0 is guaranteed to be stable and E^* does not exist (upper left region). If R^i is sufficiently small and τ suitably large, then E_0 is guaranteed to be unstable and E^* exists. The exact threshold lies between the two regions.

Fig. 3 shows how the concentration for each variable changes with time in the absence of therapy. Under the parameters above, $R_0 = 3.6114 > 1$, which implies that the virus will persist.

First, we examine the case of perfect adherence. Suppose the dosing interval is fixed at $\tau = 0.5$; that is, drugs are taken twice a day (Castagna et al., 2005). Then, according to Theorem 4.2, we have two dosage thresholds $R_1 = 0.017$ and $R_2 = 0.0103$. Fig. 4 illustrates the outcomes for $R^i = 0.01 < R_2$. Since the dosage is small, the virus dominates. Fig. 5 shows the outcomes for dosage $R^i = 0.02 > R_1$. The virus is controlled, since the dosage is sufficiently large.

Fig. 6 shows the outcomes when R^i is located between R_1 and R_2. We choose $R^i = 0.011$, 0.0135 and 0.015 respectively, satisfying $R_2 < R^i < R_1$. In the first case, the virus dominates. In the second and the third cases, the virus is controlled. Thus, the eradication threshold falls somewhere between R_1 and R_2. We observed no qualitatively different behaviours in this range that were not observed for $R^i < R_2$ or $R^i > R_1$.

Next, we examine the case of partial adherence for our model (Bartlett, 2002). This corresponds to a fixed dosage but varying dosing interval. Here, we assume that all the parameters for the immune system and virus are as above. All parameters are chosen as in Fig. 5 except that the individual takes drugs for 10 days, then stops therapy for another 10 days, and so on. The results are illustrated in Fig. 7. In this case, the virus dominates, unlike the case for perfect adherence (Fig. 5).

We also examined the effects of increasing the length of drug holidays and the intervals between them. All parameters are chosen as in Fig. 4. Figs. 8 and 9 compare no therapy, perfect adherence, and partial adherence. In Fig. 8, the latter strategy consisted of 15 days of therapy followed by a 15 day drug holiday. In Fig. 9, the partially adherent strategy consisted of 30 days of therapy followed by a 60 day drug holiday. In this case, due to sustained oscillations, the effect of partial adherence can be worse than no therapy and can also be as good as perfect adherence, depending on the length of drug holidays. That is, the viral load with partial adherence is sometimes significantly higher than the viral load without therapy and sometimes equal to the viral load with perfect adherence. Simulations show that the system has similar behaviour even if R_0 is quite high.

Additionally, we plotted the time-course of drug concentration in plasma with dose $R^i = 0.01$ under dosing interval $\tau = 0.5$ day (Fig. 10A). The time-course of the threshold $\tilde{R}_0$ with dosage $R^i = 0.01$ under dosing interval $\tau = 0.5$ day is plotted in Fig. 10B.

Finally, we explored variation in some uncertain parameters. Fig. 11 gives the graph of R_0 as a function of n (the rate of production of virions per infected cell) and a (exposure rate of gp41 after the first step). These illustrate the change of the threshold parameter R_0 as n and a vary. We also give the graph of R_0 as a function of d_1 and d_2, and contours of parameters β_1 and k. Clearly, if a and n are small, or d_1 and d_2 are large, or β_1 and k are small, then R_0 can be less than 1. Conversely, if a and n are both very large, or if d_1 and d_2 are both very small, or if k and β_1 are both large, then R_0 can blow up. For other values of the parameters, however, R_0 is relatively stable with respect to variations.

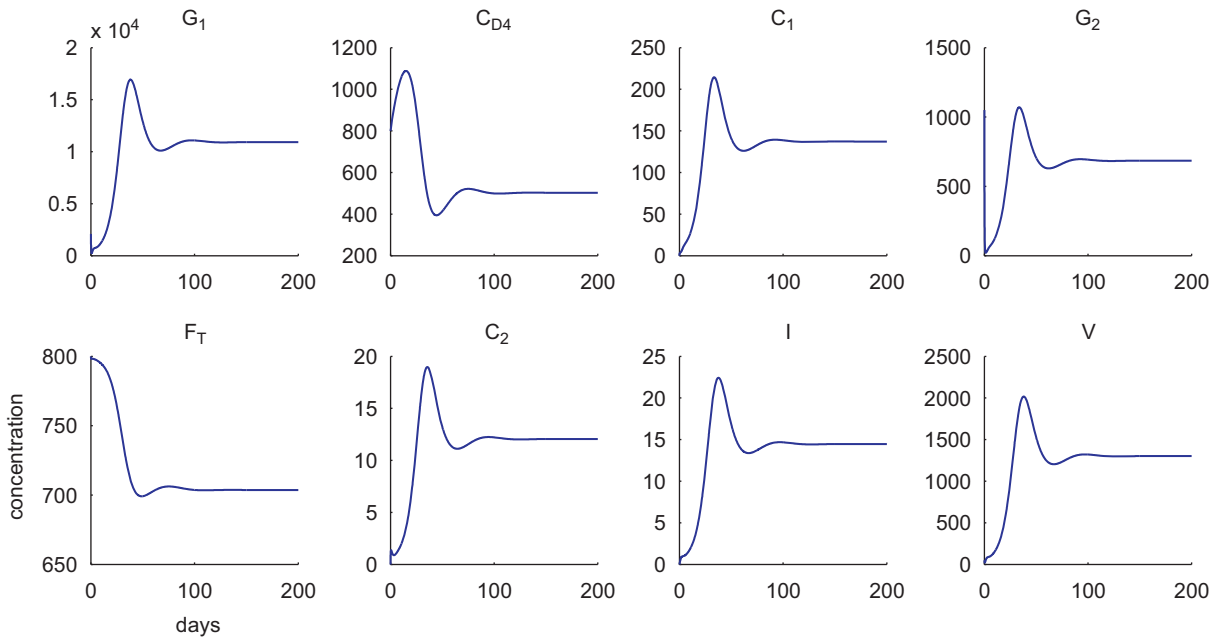

Fig. 3. Concentration changes with time in the absence of therapy. Parameter values used were as in Table 1. Initial conditions were $G_1(0)=2100$, $C_{D4}(0)=800$, $C_1(0)=0$, $G_2(0)=1050$, $F_T(0)=800$, $C_2(0)=0$, $I(0)=0$ and $V(0)=50$. With these parameters, we have $R_0=3.6114$ and hence the disease-free equilibrium is unstable and the endemic equilibrium stable.

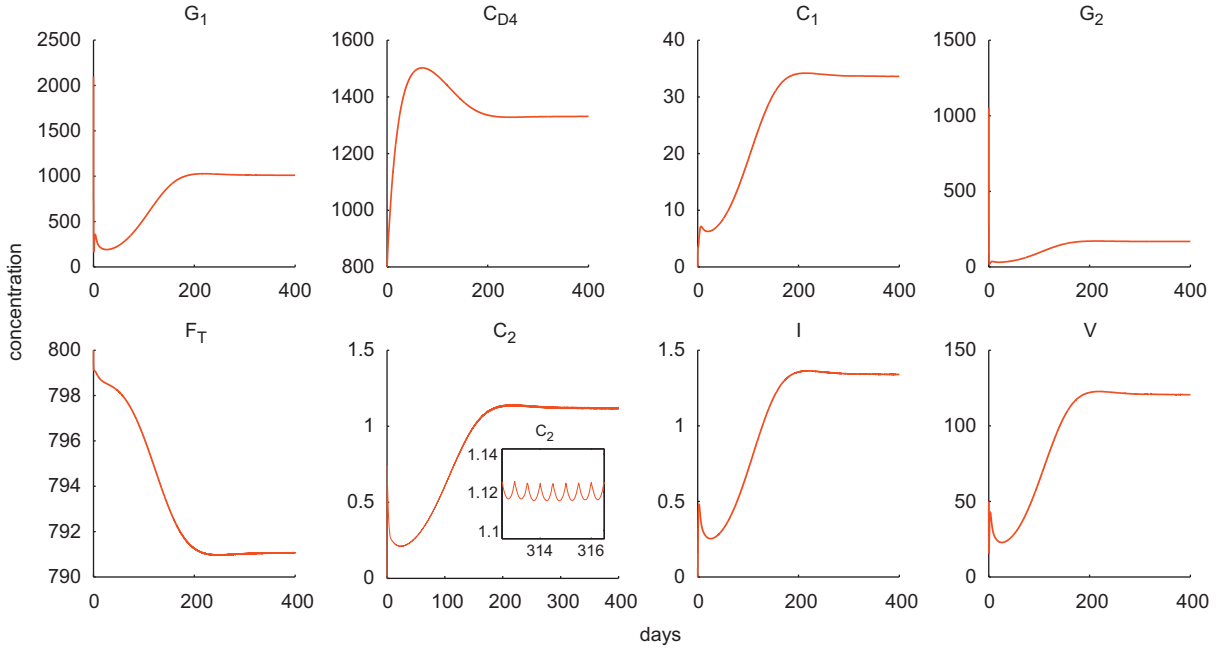

Fig. 4. Concentration changes with time under low dosage. All parameters used were the same as in Fig. 3, except $g=1$, $IC_{50}=0.01$, $\tau=0.5$ and $R^i=0.01<R_2=0.0103$; these values correspond to Sample value 1 in Fig. 2. In this case, the disease-free orbit is unstable and the endemic orbit is stable. Note that the C_2 values are significantly lower than those in Fig. 3. Inset: Since the drug is oscillating, the other state variables also oscillate, although the amplitude is small.

6. Discussion

For a sufficiently large dosage or a sufficiently small dosing interval, regular dosing of the fusion inhibitor enfuvirtide can theoretically eradicate viral infection. However, if patients are less than perfectly adherent, the result may be moderate-level persistence of the infection. If the lengths of the partially adherent intervals grow longer, then the oscillations grow larger. Consequently, a partially adherent patient may at times have a higher viral load than a patient who is not undergoing treatment; at other times, this patient may have a viral load equal to a patient who is perfectly adherent.

It should be noted that we have examined the case for enfuvirtide monotherapy. While few antiretroviral drugs are taken alone, enfuvirtide is currently prescribed as salvage treatment, when all other regimens have failed (Clotet et al., 2004). However, some patients may be taking enfuvirtide in combination with other drugs; thus, our results here for enfuvirtide monotherapy represent the most extreme case.

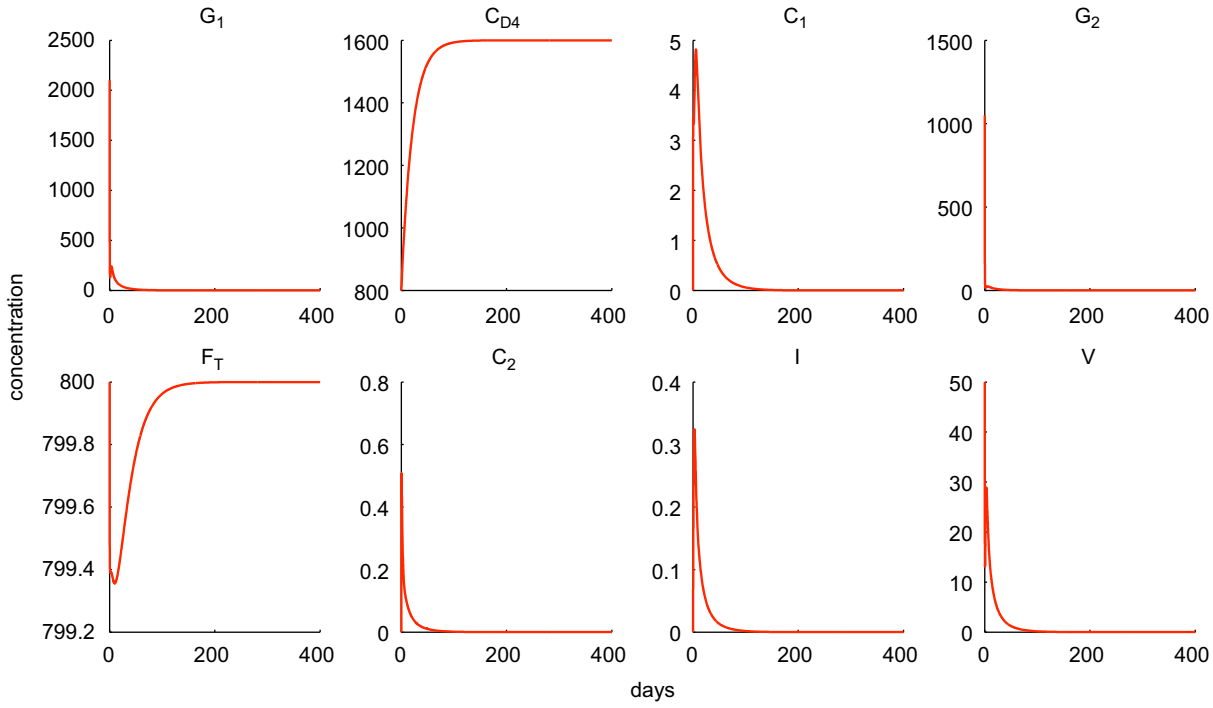

Fig. 5. Concentration changes with time under high dosage. All other parameters used were the same as in Fig. 4, with a fixed dosing interval $\tau = 0.5$. In this figure, we choose dosage $R^i = 0.02 > R_1 = 0.017$; these values correspond to Sample value 2 in Fig. 2. In this case, the disease-free orbit is stable and the endemic orbit does not exist.

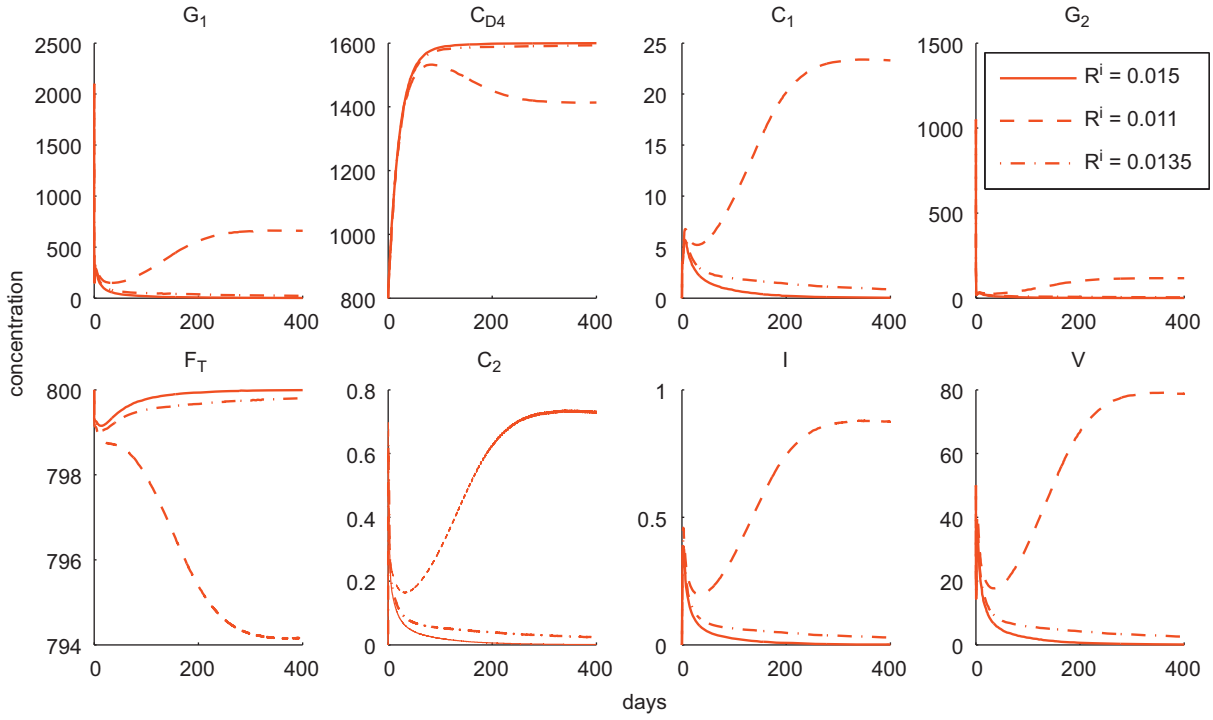

Fig. 6. Concentration changes with time under moderate dosage. All parameters used were the same as Fig. 5, except that the dosage is $R^i = 0.011$, 0.0135 and 0.015 respectively, satisfying $R_2 < R^i < R_1$. In the first case, the virus dominates. In the second and the third cases, the virus is controlled.

For some uncertain parameters, we examined their influence on R_0. For some situations, R_0 can be quite high. However, it is also possible to control the virus for appropriate therapy strategies, which suggests that enfuvirtide monotherapy can be quite useful, if applied strategically.

The model has several limitations, which should be acknowledged. First, the mechanism of drug interaction is not instantaneous. However, impulsive differential equations have been shown to be a reasonable approximation to the uptake of drug intake, provided the time between doses is not too small (Smith, 2006; Smith and Wahl, 2005). We also assumed that the growth rate of G_2 (the concentration of gp41) was directly proportional to C_1 (the combination of gp120 and CD4 receptor), which is likely a simplification. Furthermore, β_2 (the bonding force between gp41 and the CD4 receptor)

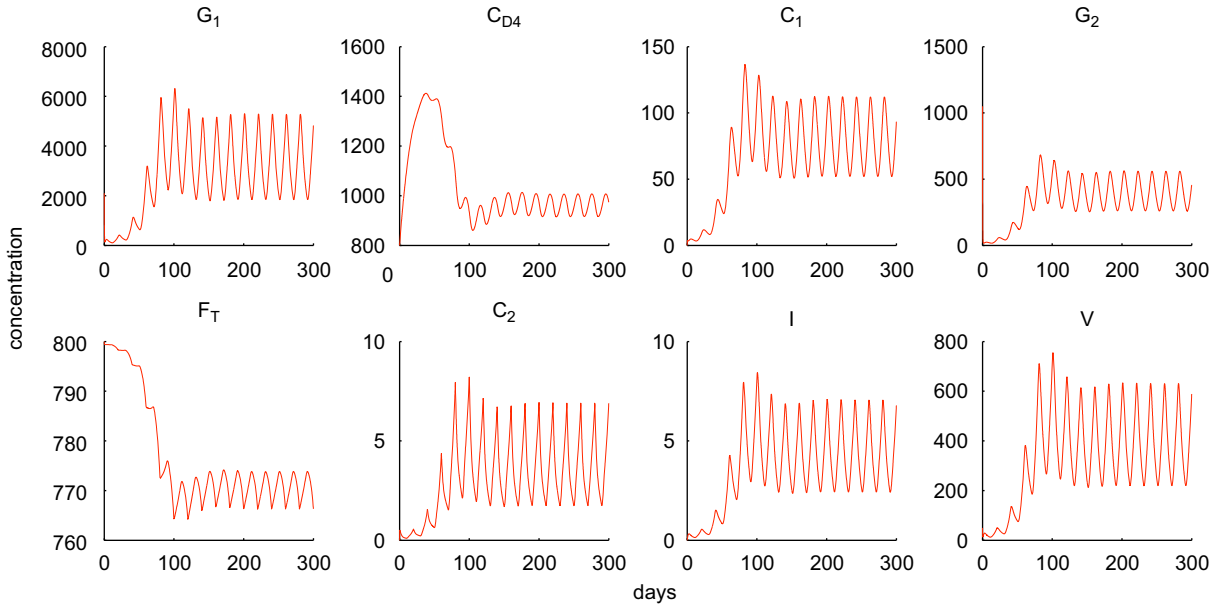

Fig. 7. Concentration changes with time under partial adherence. Here, drugs are taken for intervals of 10 days and then therapy is stopped for intervals of 10 days. All other parameters were the same as in Fig. 5. The outcome shows that, unlike perfect adherence (Fig. 5), infection cannot be cleared under this partially adherent strategy.

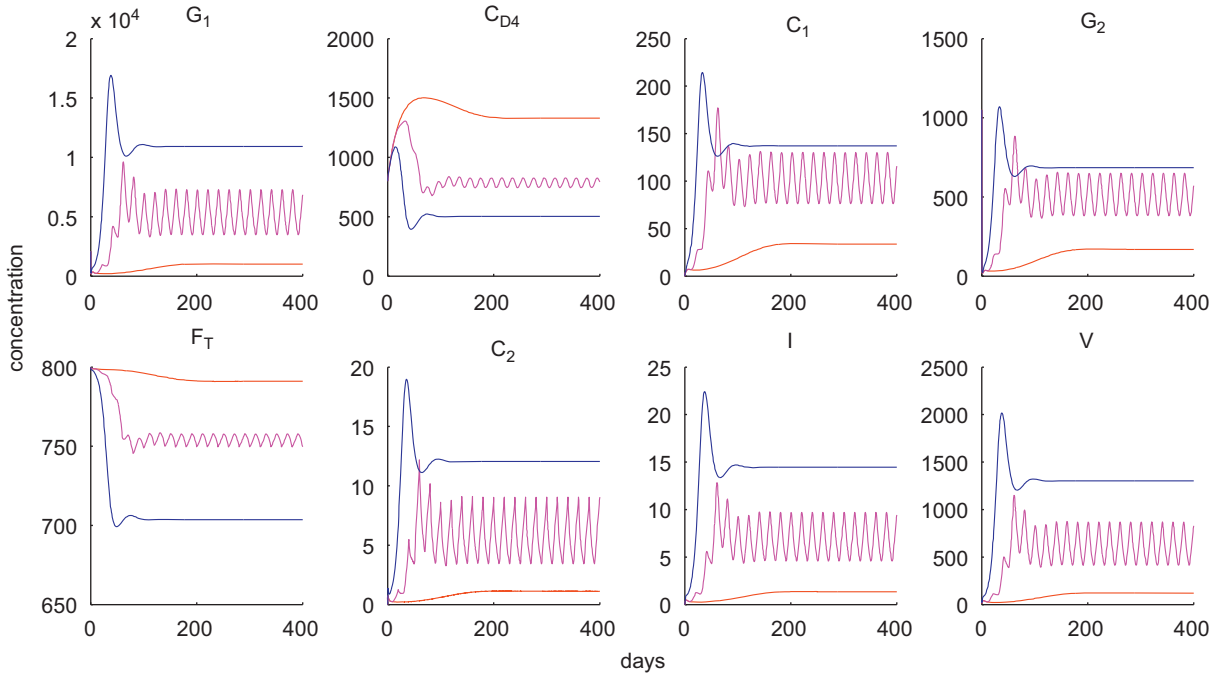

Fig. 8. Concentration changes with time under three different therapy strategies. All parameters used were the same as in Fig. 4. The oscillating curve shows the outcome when drugs are taken for intervals of 15 days and then stopped for intervals of 15 days. The dashed upper curve (lower in the C_{D4} and F_T graphs) shows the outcome without therapy. The dotted lower curve (upper in the C_{D4} and F_T graphs) shows the outcome for perfect adherence. Thus, the effect of this partially adherent strategy is between that of no therapy and perfect adherence.

probably depends on C_1, but we have assumed that it is constant. Finally, we assumed that the production of newly infected cells was directly proportional to C_2 (the combination of gp41 and the fusion protein), whereas the reality may be more complicated.

The commonly accepted viral dynamic models for antiretroviral drug therapy with reverse transcriptase or protease inhibitors integrate the dynamics of infected cells and free virions. The drug molecules prevent the virion from reproducing after it has entered the cell. Fusion inhibitors act differently. They prevent the virion from entry into the target cell by binding to viral surface proteins. On the virion's surface, there are some places to which the fusion inhibitor molecules can bind—namely, on the envelope proteins—and they make a trimer nonfunctional. There are some studies that argue that virions can only enter a cell if they harbour a minimal number of functional trimers (ranging from 2 to 19) (Sougrat et al., 2007; Klasse, 2007; Magnus et al., 2009). Zhu et al. (2006) found that HIV virions harbor only 14 ± 7 Env trimers (range 4–35). That means that the number of fusion

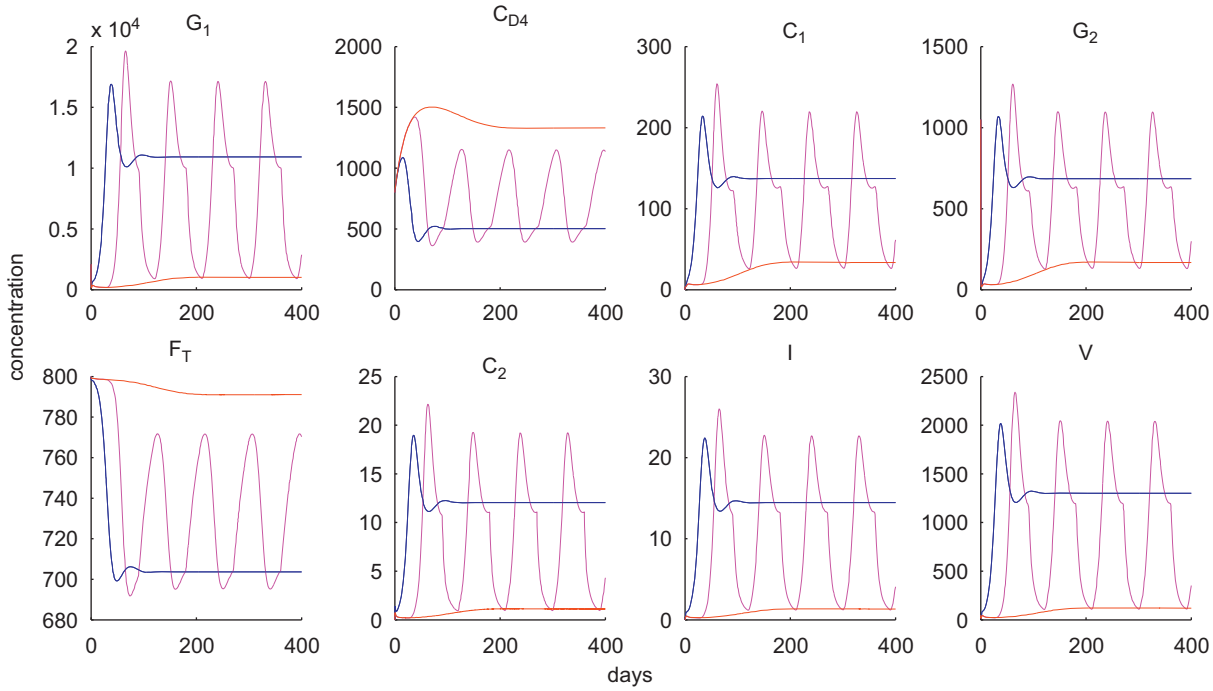

Fig. 9. Concentration changes with time under three different therapy strategies. All parameters used were the same as in Fig. 4. The oscillating curve shows the outcome when drugs are taken for intervals of 30 days and then stopped for intervals of 60 days. The nonoscillating upper curve (lower in the C_{D4} and F_T graphs) shows the outcome without therapy. The nonoscillating lower curve (upper in the C_{D4} and F_T graphs) shows the outcome for perfect adherence. Thus, the effects of this partially adherent strategy can sometimes be significantly worse than no therapy at all and at other times can be equal to perfect adherence.

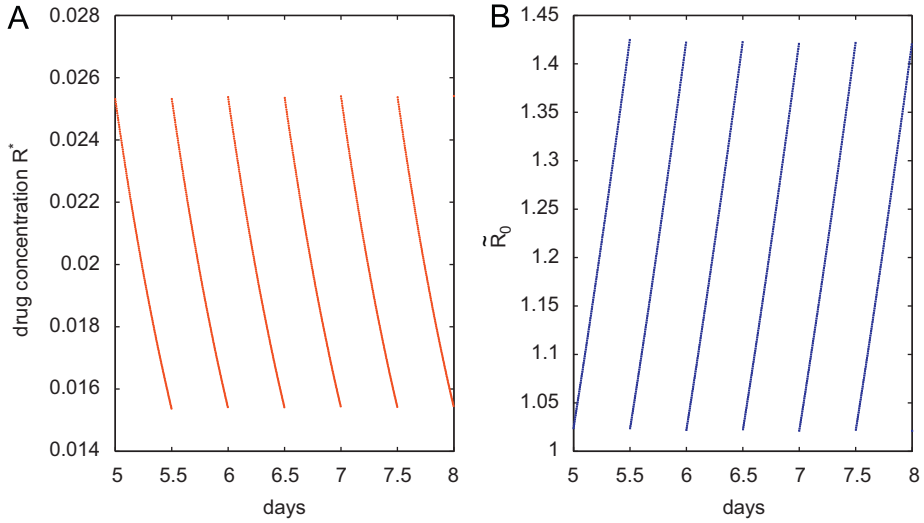

Fig. 10. (A) The time-course of drug concentration in plasma with dose $R^i=0.01$ under dosing interval $\tau=0.5$ day. (B) The time-course of the threshold $\tilde{R}_0$ with dosage $R^i=0.01$ under dosing interval $\tau=0.5$ day.

inhibitor molecules preventing one virion from entering the cell is dependent on the number of trimers on its surface. For simplicity, we assumed that HIV virions harboured 14 Env trimers in our simulations.

We chose biologically realistic initial conditions, but it should be noted that impulsive differential equations, like ordinary differential equations, could have qualitatively different results with different initial conditions. For regions where we have global stability, this is obviously not an issue, but variations in initial conditions in the middle region could produce different outcomes.

For Fig. 2, we varied R^i in order to demonstrate that the two theoretical outcomes were possible. Thus, we chose R^i values close to the analytical thresholds. However, in reality, the R^i values for enfuvirtide are 4.59 μg/mL and the drug is taken twice a day (Castagna et al., 2005). Thus, if the drug is taken as prescribed, then the outcome should fall comfortably within the region of global stability of the disease-free equilibrium. However, as adherence lapses, the dose remains constant, but the period between doses increases. In this case, the dosage/dosing-interval combination moves to the right. For short lapses in adherence, our results still predict global stability of the disease-free equilibrium. However, as the dosing interval increases, the outcome enters the region of uncertainty, where the disease-free orbit will eventually become unstable (Figs. 7–9).

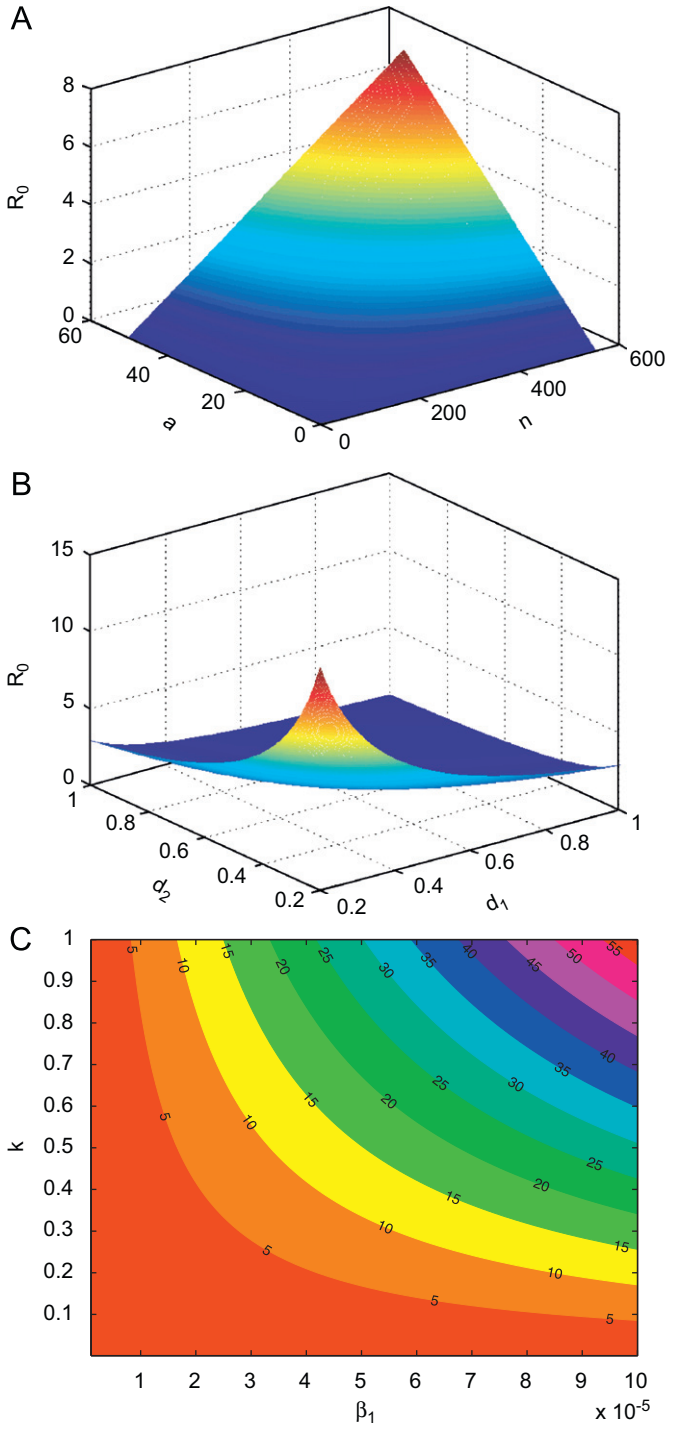

Fig. 11. (A) The graph of R_0 as a function of n and a. (B) Graph of R_0 as a function of d_1 and d_2. (C) Contour plots of R_0 as a function of β_1 and k.

It should be noted that, as with many HIV models, our results involve the theoretical eradication of the disease. However, in reality, HIV drug treatment does not eradicate the disease. This is because HIV has other reservoirs, such as the brain, eyes, testicals, etc., as well as latently infected cells, from which to re-emerge once it is controlled below the level of detection. However, our model and other similar models deal with the large-scale reductions in viral load, which can be reasonably approximated by differential equations. At a finer scale where eradication is possible, the mechanics of differential equations break down (e.g. the mass-action assumption for infection). Consequently, "theoretical eradication" in a mathematical model should be understood to mean significant reduction, below the level of detection, but not actual eradication. See Smith and Aggarwala (2009) for more discussions.

Future work will examine the effects of drug resistance, take into account the stochastic variation of parameters and consider the effects of partial adherence to enfuvirtide in combination therapy with other antiretroviral drugs.

It follows that, with regular adherence, enfuvirtide monotherapy can be effective at controlling the virus. However, as adherence lapses, the resulting oscillations may result in extreme variations, with effects that are equal to therapy at its best or significantly worse than no therapy at all. With periods of high viral load, the chances of resistant virus emerging are significantly higher. Furthermore, patients who transmit the disease during this period have a much higher probability of infecting their sex partners. Hence, we recommend that patients be counselled on the importance of adherence to this new antiretroviral drug.

Acknowledgements

We thank Shoshana Magnet, Jennifer Smith, Abba Gumel and Yang Kuang for technical discussions. We are also grateful to two reviewers whose comments greatly improved the manuscript. J.L. is supported by the Natural Science item of China under Grant no. 10701053, and Shanghai Leading Academic Discipline Project S30104. R.J.S.? is supported by an NSERC Discovery grant, an Early Researcher award and funding from MITACS. This work was also carried out with the aid of a grant (number 104519-010) from the International Development Research Center, Ottawa, Canada.

References

Bartlett, J.A., 2002. Addressing the challenges of adherence. J. Acq. Immun. Def. Synd. 29 (Suppl. 1), 2–10.
Castagna, A., Biswas, P., Beretta, P., Lazzarin, A., 2005. The appealing story of HIV entry inhibitors from discovery of biological mechanisms to drug development. Drugs 65 (7), 879–904.
Clotet, B., Raffi, F., Cooper, D., Delfraissy, J.-F., Lazzarin, A., Moyle, G., Rockstroh, J., Soriano, V., Schapiro, J., 2004. Clinical management of treatment-experienced, HIV-infected patients with the fusion inhibitor enfuvirtide: consensus recommendations. AIDS 18, 1137–1146.
Fätkenheuer, G., Pozniak, A., Johnson, M., Plettenberg, M.A., Staszewski, S., Hoepelman, I.M., Saag, M., Goebel, F., Rockstroh, J., Dezube, B., Jenkins, T.M., Medhurst, C., Sullivan, J.F., Ridgway, C., Abel, C., Youle, M., van der Ryst, E., 2004. Evaluation of dosing frequency and food effect on viral load reduction during short-term monotherapy with UK-427,857, a novel CCR5 antagonist. In: 15th International AIDS Conference, Bangkok.
Greenberg, M.L., Cammack, N., 2004. Resistance to enfuvirtide, the first HIV fusion inhibitor. J. Antimicrob. Chemother. 54, 333–340.
Hardy, H., Skolnik, P.R., 2004. Enfuvirtide, a new fusion inhibitor for therapy of human immunodeficiency virus infection. Pharmacotherapy 24 (2), 198–211.
He, X., 2006. Medical Immunology. People's Medical Publishing House, Beijing.
Heffernan, J.M., Smith, R.J., Wahl, L.M., 2005. Perspectives on the basic reproductive ratio. J. R. Soc. Interface 2 (4), 281–293.
Hethcote, H.W., 2000. The mathematics of infectious disease. SIAM Rev. 42 (4), 599–653.
Huang, Y., Rosenkranz, S.L., Wu, H., 2003. Modeling HIV dynamics and antiviral response with consideration of time-varying drug exposures, adherence and phenotypic sensitivity. Math. Biosci. 184, 165–186.
Jamjian, M.C., McNicholl, I.R., 2004. Enfuvirtide: first fusion inhibitor for treatment of HIV infection. Am. J. Health-Syst. Pharm. 61 (12), 1242–1247.
Klasse, P.J., 2007. Modeling how many envelope glycoprotein trimers per virion participate in human immunodeficiency virus infectivity and its neutralization by antibody. Virology 369 (2), 245–262.
Krakovska, O., Wahl, L.M., 2007. Optimal drug treatment regimens for HIV depend on adherence. J. Theor. Biol. 246, 499–509.
Levy, J., 2007. HIV and the Pathogenesis of AIDS. American Society for Microbiology, Washington DC.
Liu, H., Li, L., 2010. A class age-structured HIV/AIDS model with impulsive drug-treatment strategy. Discrete Dynamics in Nature and Society (Article ID 758745).
Liu, H., Yu, J., Zhu, G., 2008. Global behaviour of an age-infection-structured HIV model with impulsive drug-treatment strategy. J. Theor. Biol. 253, 749–754.

Liu, S.-W., Wu, S.-G., Jiang, S.-B., 2005. Advancement in developing a new class of anti-AIDS drugs: HIV entry inhibitors. Chin. Pharmacol. Bull. 21 (9), 1034–1040.

Magnus, C., Rusert, P., Bonhoeffer, S., Trkola, A., Regoes, R.R., 2009. Estimating the stoichiometry of human immunodeficiency virus entry. J. Virol. 83(3), 1523–1531.

Magombedze, G., Garira, W., Mwenje, E., 2008. Modelling the immunopathogenesis of HIV-1 infection and the effect of multidrug therapy: the role of fusion inhibitors in HAART. Math. Biosci. Eng. 5 (3), 485–504.

Mohanty, U., Dixit, N.M., 2008. Mechanism-based model of the pharmacokinetics of enfuvirtide, an HIV fusion inhibitor. J. Theor. Biol. 251, 541–551.

Miron, R.E., Smith?, R.J., 2010. Modelling imperfect adherence to HIV induction therapy. BMC Infect. Dis. 10, 6.

Moyle, G., 2003. Stopping HIV fusion with enfuvirtide: the first step to extracellular HAART. J. Antimicrob. Chemother. 51, 213–217.

Perelson, A.S., Kirschner, D.E., de Boer, R., 1993. Dynamics of HIV infection of $CD4^+$ T cells. Math. Biosci. 114, 81–125.

Smith, R.J., 2006. Adherence to antiretroviral HIV drugs: how many doses can you miss before resistance emerges? Proc. R. Soc. B 273 617–624.

Smith, R.J., Wahl, L.M., 2004. Distinct effects of protease and reverse transcriptase inhibition in an immunological model of HIV-1 infection with impulsive drug effects. Bull. Math. Biol. 66 (5), 1259–1283.

Smith, R.J., Wahl, L.M., 2005. Drug resistance in an immunological model of HIV-1 infection with impulsive drug effects. Bull. Math. Biol. 67, 783–813.

Smith?, R.J., Aggarwala, B.D., 2009. Can the viral reservoir of latently infected $CD4^+$ T cells be eradicated with antiretroviral HIV drugs? J. Math. Biol. 59 697–715.

Sougrat, R., Bartesaghi, A., Lifson, J.D., Bennett, A.E., Bess, J.W., Zabransky, D.J., Subrmaniam, S., 2007. Electron tomography of the contact between T cells and SIV/HIV-1: implications for viral entry. PLoS Pathog. 3 (5), e63.

Tardif, M.R., Tremblay, M.J., 2005. Regulation of LFA-1 activity through cytoskeleton remodeling and signaling components modulates the efficiency of HIV Type-1 entry in activated $CD4^+$ T lymphocytes. J. Immunol. 175, 926–935.

Tsai, L., Trunova, N., Gettie, A., Mohri, H., Bohm, R., Saifuddin, M., Cheng-Mayer, C., 2007. Efficient repeated low-dose intravaginal infection with X4 and R5 SHIVs in rhesus macaque: implications for HIV-1 transmission in humans. Virology 362, 207–216.

Trottier, B., Walmsley, S., Reynes, J., Piliero, P., O'Hearn, M., Nelson, M., et al., 2005. Safety of enfuvirtide in combination with an optimized background of antiretrovirals in treatment-experienced HIV-1-infected adults over 48 weeks. J. Acq. Immun. Def. Synd. 40 (4), 413–421.

van den Driessche, P., Watmough, J., 2002. Reproduction numbers and subthreshold endemic equilibria for compartmental models of disease transmission. Math. Biosci. 180, 29–48.

Wahl, L.M., Nowak, M.A., 2000. Adherence and drug resistance: predictions for therapy outcome. Proc. R. Soc. London B 267, 835–843.

Yadav, V., Balakrishnan, S.N., 2006. Optimal Impulse control of systems with control constraints and application to HIV treatment. In: Proceedings of the 2006 American Control Conference Minneapolis, Minnesota, USA, June 14–16, 2006, pp. 4824–4829.

Zhu, P., Liu, J., Bess, J., Chertova, E., Lifson, J.D., Grise, H., Ofek, G.A., Taylor, K.A., Roux, K.H., 2006. Distribution and three-dimensional structure of AIDS virus envelope spikes. Nature 441, 847–852.